Available online at www.sciencedirect.com
ScienceDirect
Chemical Geology 245 (2007) 254–274
CHEMICAL GEOLOGY INCLUDING ISOTOPE GEOSCIENCE
www.elsevier.com/locate/chemgeo

Porewater redox species and processes in the Black Sea sediments

Sergey K. Konovalov [a,*], George W. Luther III [b], Mustafa Yücel [b]

[a] *Marine Hydrophysical Institute, Sevastopol 99011, Ukraine*
[b] *College of Marine and Earth Studies, University of Delaware, Lewes, DE 19958, USA*

Received 11 April 2007; received in revised form 20 August 2007; accepted 25 August 2007

Editor: D. Rickard

Abstract

During the 2003 KNORR and the 2005 ENDEAVOR cruises to the Black Sea, voltammetric solid-state microelectrode data were collected for the vertical distribution of redox species in porewaters from the upper 200 to 300 mm layer of sediments with mm vertical resolution. We discuss vertical distributions of dissolved sulfide, manganese and iron species in sediments from the oxic, suboxic, anoxic/sulfidic parts of the Black Sea. Results of voltammetric profiling demonstrate many processes governing the porewater chemistry of oxic shelf sediments, suboxic shelf slope sediments, deep anoxic sediments (Unit I), and turbidites in deep anoxic sediments.

Sediments from the oxic shelf areas appear to be spatially similar in their porewater chemistry revealing the same sequence of redox species, as elsewhere in the Ocean, except for the lack of manganese. This lack of manganese is explained by its diagenetic remobilization and accumulation in anoxic waters and suboxic sediments. Sediments from the suboxic part of the shelf slope reveal high concentrations of manganese (II) and iron (II) in porewaters. Still, the flux of Mn(II) from these sediments comprises only a part of the Mn(IV) that precipitates from the water column and can be diagenetically recycled in these sediments. These sediments appear to be the major net sink of manganese as it is not accumulated in sediments of either the oxic or anoxic parts of the Sea. The porewater chemistry of deep anoxic cores showed major spatial variations in the magnitude and even direction of the flux of sulfide. The sediments from the eastern central Black Sea show an expected Unit 1 source of sulfide to the overlying water and have high sulfide content, up to 1600 μM. In the anoxic western and near coastal cores, turbidites cause significant loss of porewater sulfide down to nondetectable sulfide (<0.2 μM). The latter can be explained by the origin and oxidized Mn and Fe content of turbidites.

Keywords: Black Sea; Voltammetric profiling; Porewater chemistry

1. Introduction

The Black Sea is the most studied marine system which has permanent deep-water anoxia. Hundreds of publications and a number of extensive data sets describe the Black Sea's structure and evolution. This sea has become an *in situ* laboratory basin to study various biogeochemical processes and redox budgets. The Black Sea and other oxic/anoxic aquatic systems

* Corresponding author. Kapitanskaya Street, Sevastopol 99011, Ukraine.
E-mail addresses: sergey_konovalov@yahoo.com (S.K. Konovalov), luther@udel.edu (G.W. Luther), myucel@udel.edu (M. Yücel).

0009-2541/$ - see front matter © 2007 Elsevier B.V. All rights reserved.
doi:10.1016/j.chemgeo.2007.08.010

have usually been investigated for the location and variations in the depth of disappearance of O_2 and the onset of sulfide and other reduced species in the water column. Publications on the chemistry and structure of the Black Sea sediments and especially on the chemistry of porewater are more limited. One major reason is related to difficulties in collecting and analyzing undisturbed sediments and porewater. The work here partially fills this gap by presenting and discussing the novel results of voltammetric profiling which shows the distribution of dissolved sulfide, iron(II) and manganese (II) in porewaters from the upper 200 to 300 mm layer of sediments from the oxic, suboxic and sulfidic sediment regimes.

Historically, the Black Sea sediments were intensively studied by Soviet oceanographers for geological purposes starting from the 1950's (see overviews in Mitropolsky et al., 1982 and in Neprochnov et al., 1974). As the result of those studies, general geological and basic mineralogical descriptions became available (Shimkus and Trimonis, 1974). Those data were poorly resolved vertically, but the upper carbonate rich Holocene layer, iron monosulfide rich black sediments, organic carbon rich sapropels, and deeper carbon poor clay sediments were acknowledged (Strakhov, 1963; Shimkus and Trimonis, 1974; Mitropolsky et al., 1982). Spatial variations in the solid phase composition were resolved by the study of hundreds of stations across the sea (Mitropolsky et al., 1982). Iron monosulfide rich black sediments were recognized as typical for the periphery of the deep sea, while three other types of sediments (carbonate rich Holocene sediments, organic carbon rich sapropels, and deeper carbon poor clay sediments) were identified for the central deep part of the sea. Strakhov (1963) and Volkov (1964) were likely the first to discuss diagenetic processes and specifically the sulfidization of iron in Black Sea sediments (Volkov and Fomina, 1974; Rozanov et al., 1974; Pilipchuk and Volkov, 1974).

Results of coring during the 1969 ATLANTIS expedition to the Black Sea made sediments widely available for analysis and data interpretation (Ross et al., 1970; Degens and Ross, 1972; Berner, 1974). While turbidites (FeS black homogeneous sediments) were acknowledged for the eastern periphery of the deep sea, major attention was paid to three-layer sediments (Unit I — carbonate rich Holocene layer, Unit II — organic carbon rich sapropels and Unit III — deeper organic carbon-limited clay sediments) in the central part of the sea (Degens and Ross, 1972). Unit I is a 200 to 500 mm layer of carbonate rich laminated sediments which provided a unique opportunity to study sedimentation processes under anoxic conditions over a period of thousands of years (Degens and Ross, 1972; Arthur et al., 1994). It dominated almost all geochemical studies in the Black Sea for the following decades. Published porewater data were primarily available for salinity and major ions to study large-scale processes on the water and salt budget (Manheim and Chan, 1974). Data on minor and redox constituents were scarce and decoupled from information on the type and structure of sediments.

Pyrite formation and accumulation in Black sea sediments were then intensively studied (e.g.; Calvert and Karlin, 1991; Lyons and Berner, 1992; Canfield et al., 1996; Hurtgen et al., 1999; Wijsman et al., 2001a; Wilkin and Arthur, 2001; Anderson and Raiswell, 2004; Neretin et al., 2004). The key questions addressed were limited to variations in the degree of pyritization within the cores of euxinic sediments and the importance of syngenetic vs. diagenetic production of pyrite (Lyons, 1997; Wilkin et al., 1997), to S–C–Fe systematics (Calvert and Karlin, 1991; Lyons, 1997; Wilkin and Arthur, 2001), and to sources and mechanisms for the enrichment of highly reactive iron, primarily in the form of pyrite, in euxinic Black Sea sediments (Anderson and Raiswell, 2004). Though the importance of elemental sulfur, polysulfides, and sulfide for pyritization was either discussed (Hurtgen et al., 1999) or assumed, speciation data were traditionally limited to solid phases in Units I, II, and III. Turbidites, though acknowledged (Strakhov, 1963; Ross et al., 1970), were usually discussed in terms of their origin and deposition in the Danube deep-sea fan (Popescu et al., 2001; CIESM, 2002) or in terms of differences in pyrite formation and accumulation in turbidites and Unit I (Lyons and Berner, 1992; Arthur et al., 1994; Canfield et al., 1996; Wilkin and Arthur, 2001).

Building on earlier studies on the measurement of FeS_2 alone, recent studies also included data on AVS (acid volatile sulfur, basically FeS), reactive and total iron in euxinic (Hurtgen et al., 1999; Wijsman et al., 2001b; Lyons and Kashgarian, 2005) and shelf (Thamdrup et al., 2000; Wijsman et al., 2001a,b) sediments. Available porewater data are limited to 9 profiles of sulfate, sulfide, and dissolved iron in shelf and slope sediments (Wijsman et al., 2001b) and a few profiles of sulfate and sulfide in turbidites and Unit I cores (Lyons and Berner, 1992; Hurtgen et al., 1999; Lyons and Kashgarian, 2005).

Though limited in number, these data lead to a number of questions on porewater chemistry and water–sediment interactions. Although cores of Unit I from different parts of the sea reveal an almost identical morphology and similar solid phase properties (concentration of organic and inorganic carbon, FeS_2, AVS, total and reactive iron, total sulfur, degree of pyritization, etc.), the porewater profiles of H_2S can be critically different. Lyons and

Berner (1992) published two H_2S profiles. One from the western central station (location A in Fig. 1 that is station 9, leg 4, 1988 KNORR cruise) suggested that the maximum H_2S concentration did not exceed 250 μM, which is about 150 μM below the level of sulfide in the bottom waters whereas the other profile from the central station south of the Crimea (location B in Fig. 1 that is station 14, leg 4, 1988 KNORR cruise) revealed a maximum H_2S concentration of about 700 μM. A 3-fold difference between the concentrations of sulfide in these cores was left unexplained as it did not fit the almost identical values of organic carbon, sulfate, and reactive iron. Thus, questions on the porewater chemistry and its major driving processes have remained unexplained.

Available data on turbidites also appear controversial. Turbidites were initially reported to be "extremely homogeneous in color, grain size (<2 μm), and chemistry" (Ross et al., 1970; Arthur et al., 1994). Lyons and Berner (1992) reported that the turbidites in some locations appeared homogeneous under both visual and X-radiographic examination, but in other locations muds displayed a strikingly obvious lamination when viewed by X-radiography. Lyons and Berner (1992), Arthur et al. (1994) and Canfield et al. (1996) stated that the exact process of deposition is not certain, but turbidites are "inserted" between laminae with little or no erosion assuming very low energy processes for their deposition. Available data on natural radioisotopes, degree of pyritization, and other properties suggested that turbidites originate from anoxic margins of the basin. However, available data do not explain that turbidites from two adjacent locations can be different in their properties (Wijsman et al., 2001b) while turbidites from widely spaced locations "reveal strong similarities" (Lyons and Kashgarian, 2005).

The objectives of this work are (i) to present porewater data from the upper 300 mm layer of sediments throughout the Black Sea using a voltammetric microelectrode to profile sediment cores recovered during the 2003 KNORR expedition, (ii) to discuss the porewater chemistry for different and similar types of sediments from oxic, suboxic,

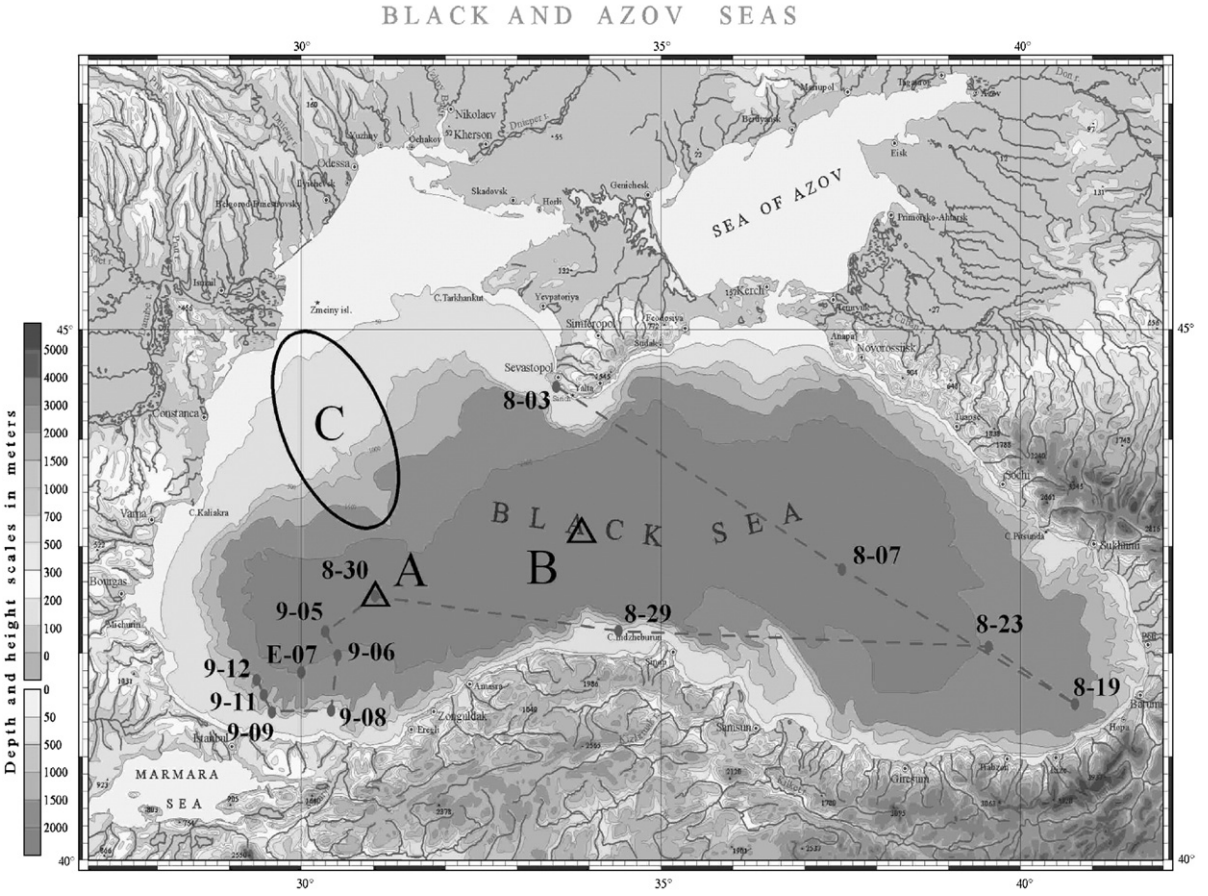

Fig. 1. The 2003 KNORR and 2005 ENDEAVOR sediment sampling sites (dots), as well as locations (empty triangles) of station 9 (A) and station 14 (B) from leg 4 of the 1988 KNORR expedition and the area (oval) of sediments (C) discussed by Thamdrup et al. (2000) and Wijsmana et al. (2002).

and sulfidic parts of the sea and (iii) to discuss the importance of sediment porewater geochemistry to water column chemistry and the budget of manganese.

2. Methods

2.1. Sample collection and voltammetric profiling methodology

Black Sea sediment cores were retrieved with a multi-corer MC-800 (Ocean Instruments Inc.) from a number of locations on the shelf, continental slope and deep part of the sea (Fig. 1) during leg 2 and leg 3 of the 2003 KNORR expedition from April 10 to May 10 (www.ocean.washington.edu/cruises/Knorr2003) and during the 2005 ENDEAVOR (www.ocean.washington.edu/cruises/Endeavor2005) expedition from March 27 to April 05 to the Black Sea. The retrieved sediment cores came from regions where sediments are exposed to permanent oxic, suboxic, or anoxic/sulfidic waters. The multi-corer allowed sampling of undisturbed sediment cores as the surface "fluff-layer" and overlying water (Fig. 2) were intact. The cores included oxic–anoxic sediments from the shallow shelf oxic areas (Fig. 2a), non-sulfidic anoxic sediments (Fig. 2b) from the shelf slope at the depth of the suboxic zone, sediments from Unit I (Fig. 2c), and finally mono- to multi-layer turbidites (Fig. 2d–f).

Voltammetric profiling (Luther et al., 1998) was immediately performed on the sediment cores to avoid changes in the core conditions except bottom-to-surface pressure changes. The usual lag-time between getting sediment cores from the deck to the start of profiling did not exceed 30 min. Data for the first profile was usually acquired within 1 h. An Analytical Instrument Systems Inc. Model DLK-60 voltammetric analyzer was used for all measurements. An Au/Hg amalgam solid-state working microelectrode was used (Brendel and Luther, 1995). An Ag/AgCl electrode was used as a reference, and a platinum wire was used as a counter electrode in a traditional 3-electrode setup. The working electrode was calibrated daily using the pilot ion method (Luther et al., 1999; Luther et al., in press). It was also shown that the calibration remained within 5% over the period of profiling.

A manually controlled mechanical micromanipulator was used to profile the sediment core with the Au/Hg amalgam solid-state microelectrode to a depth of 300–400 mm with sub-millimeter scale vertical resolution (Luther et al., 1999, 2001). Scans were normally run from −0.1 to −1.7 V in a linear sweep or cyclic voltammetry mode at the rate of 0.5 or 1.0 V/s. Scans were run in triplicate at 1 mm vertical increments. Initial data were digitized and processed with software provided by

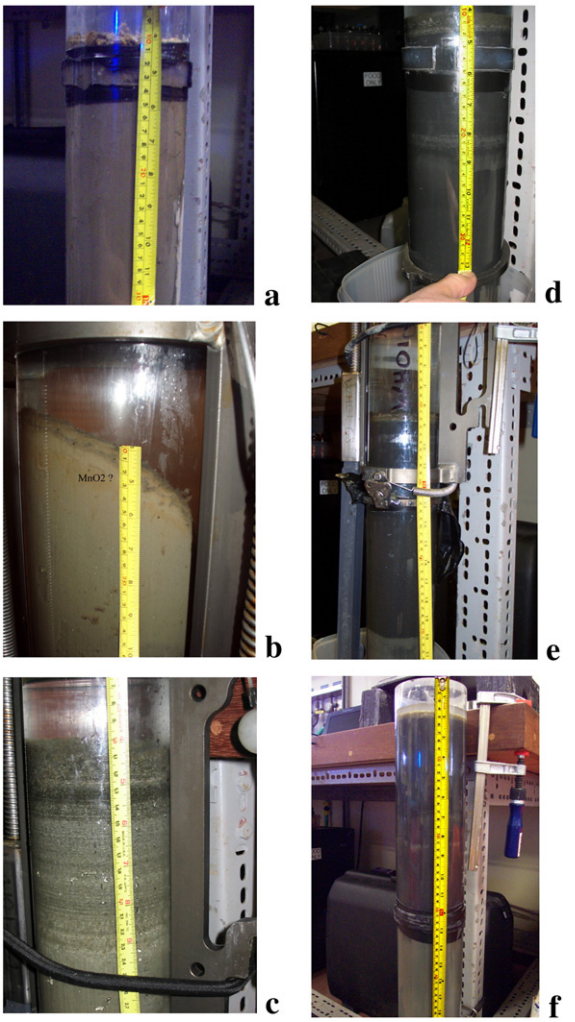

Fig. 2. Sediment cores from (a) 8-29 (oxic), (b) 9-12 (suboxic), (c) station 8-7 (anoxic Unit I), and anoxic cores containing turbidites at (d) station 8-19, (e) 9-06, (f) 9-05.

Analytical Instrument Systems Inc. The software can analyze sequences of scans (Fig. 3), reconstruct vertical profiles of individual redox species (Fig. 4), and convert linear sweep scans into derivative scans for accurate potential information (Fig. 5). The sediment cores were sliced in 10 mm thick layers after voltammetric profiling and immediately frozen at −20 °C in plastic bags or falcon tubes under argon for further on-shore analyses.

Sediment cores can be quite heterogeneous pending bioturbation, plant growth and physical mixing (Luther et al., 1998; Bull and Taillefert, 2001). At least duplicate vertical profiles (separated by 20–30 mm) were obtained on each core (e.g., Fig. 4b) to make sure that the cores were homogeneous. Individual Black Sea cores gave reproducible profiles with minor changes due to small-

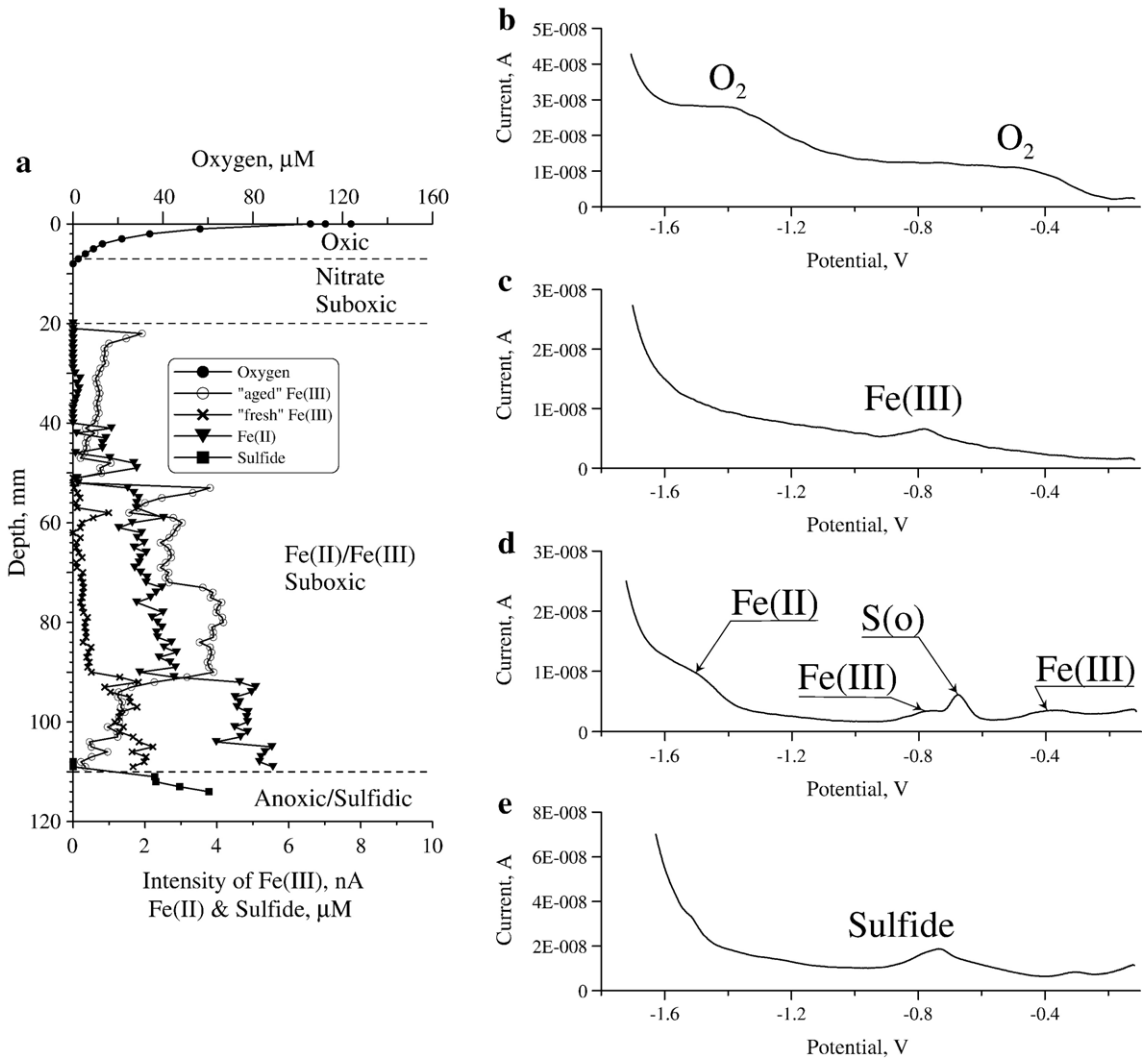

Fig. 3. Vertical profiles (a) and individual voltammetric linear scans at the depth of 2 (b), 22 (c), 93 (d), and 114 mm (e) of the oxic sediment core of station 8-03. Voltammetric scans at individual depths are shown in Fig. 5.

scale heterogeneity (for example, Figs. 4b and 6a, d, e), so basin-wide variations in the porewater chemistry can be easily compared.

2.2. Flux calculations

Data on the distribution of dissolved Mn(II) in porewater can be used to calculate its vertical flux using Eq. (1):

$$F = -D \cdot \frac{\partial C}{\partial z} + W \cdot C, \quad (1)$$

where D is a diffusion coefficient, W is the rate of advection, C is the concentration, and z is the depth.

The vertical diffusive flux (F_{diff}) is calculated using Fick's first law (Eq. (2)):

$$F_{\text{diff}} = -\varphi \cdot \frac{D_T}{(1 - \ln(\varphi^2))^2} \cdot \frac{\partial C}{\partial z}, \quad (2)$$

where φ is the porosity, D_T is the molecular diffusion coefficient corrected for the *in situ* temperature (Eq. (3)), and $(1-\ln(\varphi^2))^2$ is the tortuosity (Chaillou et al., 2007).

$$D_T = D_0 \cdot \frac{\eta_0}{\eta_T} \cdot \frac{T}{T_0}, \quad (3)$$

where D_T and η_T are the molecular diffusion coefficient and the value of water viscosity for the *in situ*

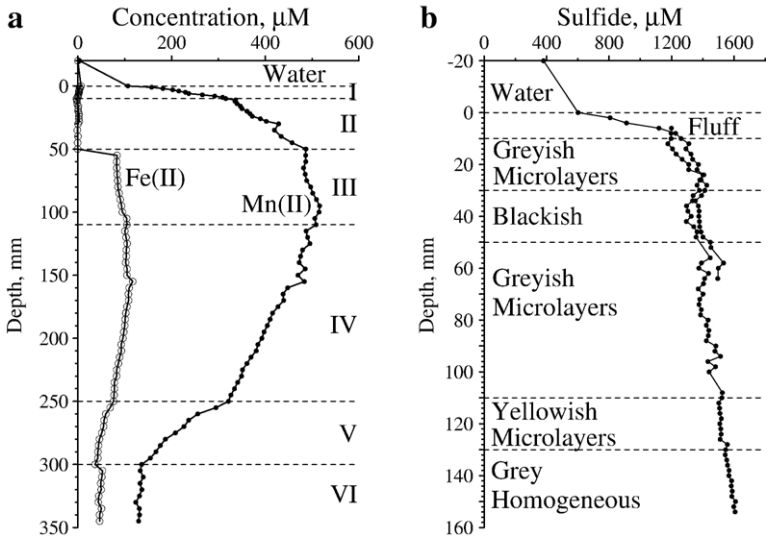

Fig. 4. Vertical porewater profiles of manganese (II) and iron (II) at station 9-12 (a) and sulfide at station 8-07 (b). The vertical profiles of Mn(II) and Fe(II) are shown in a.

temperature T and D_0 and η_0 are the molecular diffusion coefficient and the value of water viscosity for the known temperature T_0.

Assuming the profile of Mn(II) is at a steady state, the rate of advection can be estimated as the rate of sediment deposition, which is equal to 0.2 mm/yr for sediments from the shelf slope (Mitropolsky et al., 1982). The calculated profile of Mn(II) has been fitted to the observed data (Fig. 7a). The diffusion coefficient D_0 (Mn^{2+} at 20 °C) = $5.44 \cdot 10^{-6}$ cm^2/s (Chaillou et al., 2007) has been corrected for the *in situ* temperature (Eq. (3)). Finally, the porosity has been determined as the ratio of the volume of water in a wet sample to the volume of the sample to vary from 0.92 in the upper "fluff" layer to 0.87 at the maximum profiled depth. The resulting profile of the Mn(II) flux is presented at Fig. 7b, where negative values indicate the flux is directed upward, while positive values indicate a downward flux.

3. Results

3.1. Sediment morphology and its spatial variations

The first major observation based on visual analysis of the sediment cores (Fig. 2) is that the Black Sea sediments appear very variable. Spatial and temporal variations in the chemical structure of the Black Sea water column have been discussed (Konovalov and Murray, 2001; Konovalov et al., 2003; Glazer et al., 2006), but the chemistry of the upper layer of sediments and porewaters has been assumed to be more conservative (Lyons and Kashgarian, 2005). As will be shown, sediments may have different morphology and presumably mineralogy but similar porewater chemistry or sediments similar in appearance may have substantially different chemical properties as also shown by Wijsman et al. (2001b).

Another major observation is that the sediment core from the central eastern part of the sea (station 8-7, Fig. 1) is the only Unit I type. All other sediment cores from the anoxic part of the sea contain turbidites that vary in color, morphology and sediment texture, as well as porewater chemistry. The actual area, where the Unit I structure is not marred by intrusions of turbidites, is limited to the very central part of the sea, as suggested by Shimkus and Trimonis (1974) and reviewed by Mitropolsky et al. (1982).

3.2. Sediments from the oxic shelf

Oxic shelf sediments appeared to be different in their morphology and texture. Sediments from the Anatolian shelf (station 8-29, Fig. 1) were basically light brown to grey clayish material (Fig. 2a). It looked homogeneous, but had many shells and carbonate pebbles of an average diameter of 5 to 20 mm. This texture did not vary with depth within the upper 300 mm, though the upper 10 mm of the column had a mixture of "fluff" (potentially remnants of sinking organic material) and empty shells of the same size, as those deeper in the column of sediments.

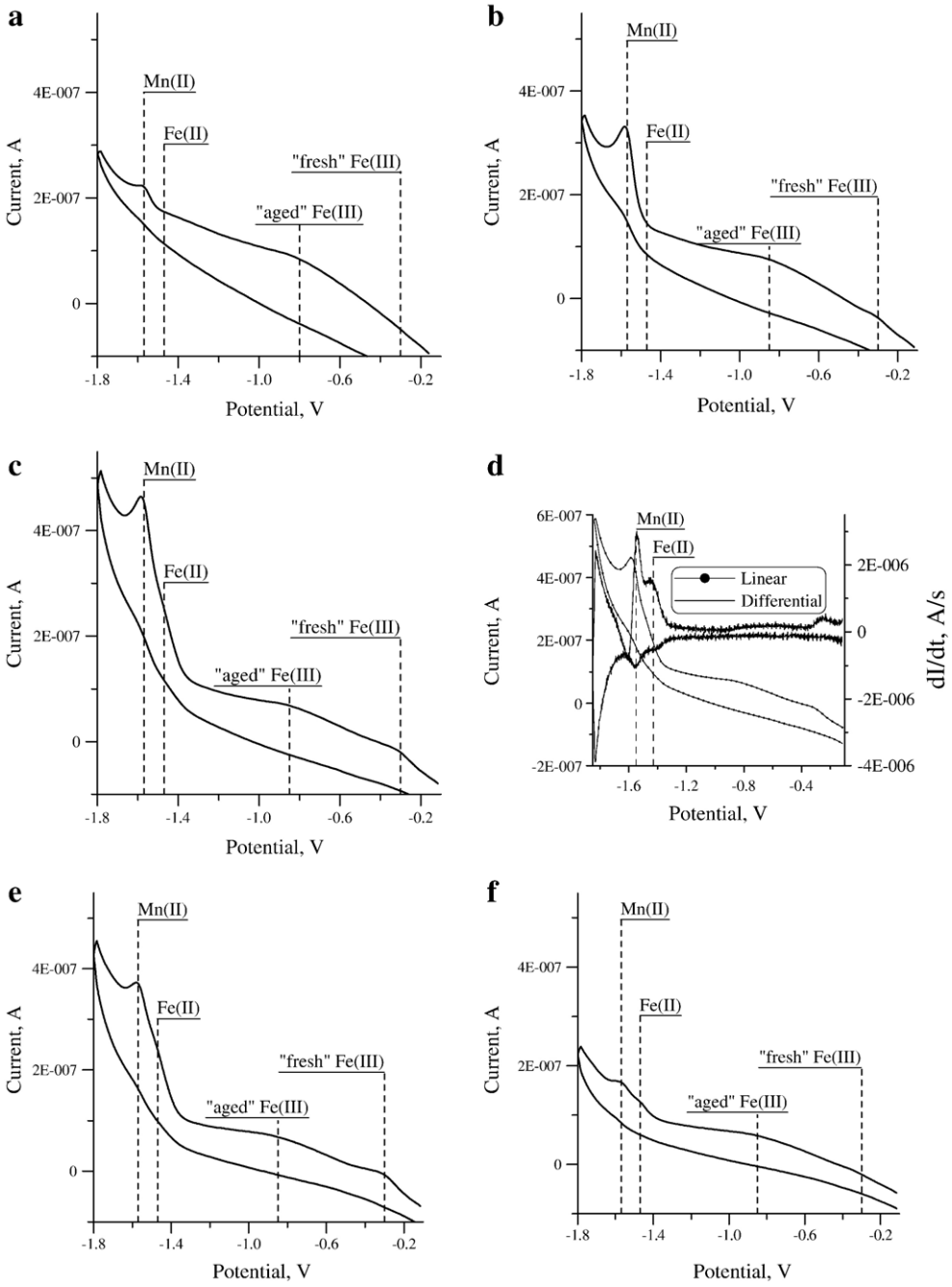

Fig. 5. Individual voltammetric linear cyclic scans at specific depths of the sediment core at station 9-12.

Sediments from the Crimean shelf (station 8-03, Fig. 1) were also clayish (picture not shown) and were covered with ~10 mm of "fluff" material. Still, these sediments were different from the Anatolian shelf as the sediments from Station 8-03 had many small shells of 1 mm and less size. This carbonate material made the sediments lighter in color. The upper 40 mm below the "fluff" material were distinctly laminated with dark and almost white layers. Individual layers became progressively less recognizable at depths between 50 and 100 mm. The sediments looked homogeneous below ~100 mm depth. Though the morphology and texture of

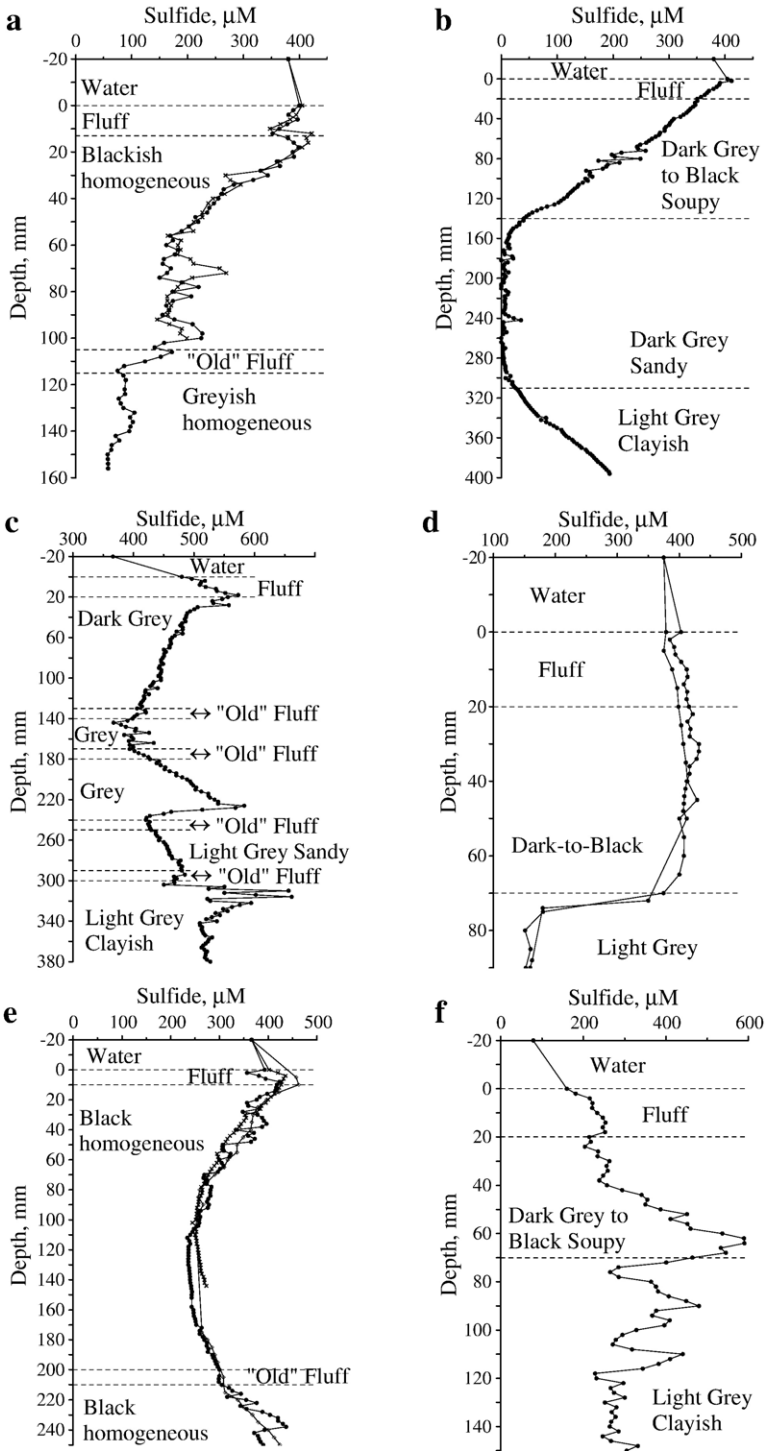

Fig. 6. Vertical profiles of sulfide in porewater of anoxic cores containing turbidites at stations 8-19 (a), 9-06 (b), 9-05 (c), 9-11 (d), 8-30 (e), and 9-08 (f).

oxic shelf sediments from different locations vary, the voltammetric scans demonstrate very similar sequences of redox species.

The overlying waters are oxygen saturated, but oxygen penetrated 6–8 mm into the sediments. This upper layer is called “oxic” (Fig. 3a,b). The deeper

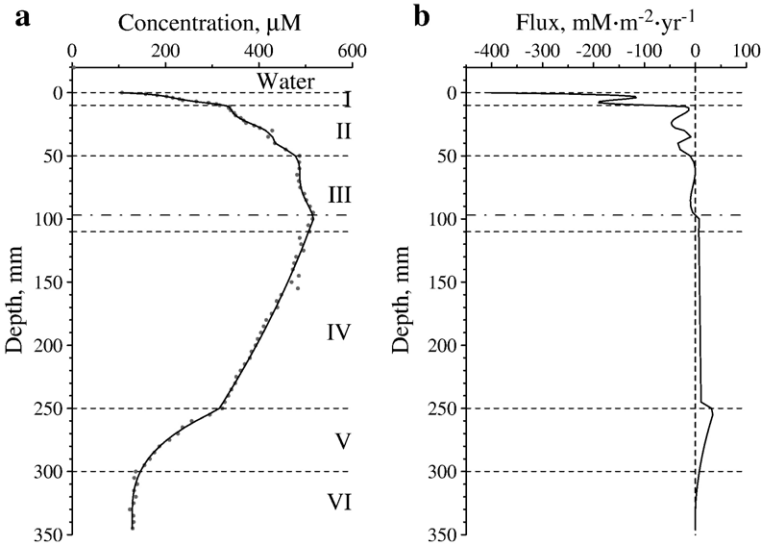

Fig. 7. The vertical profile of Mn(II) in porewaters of the suboxic sediments fitted for observed data (a) and the calculated profile of the flux of Mn(II) (b).

"nitrate suboxic" layer from 6 to 20 mm (Fig. 3a) does not reveal any voltammetric signals (Fig. 3c). Redox processes in this layer are presumably controlled by nitrogen transformations from nitrate to N_2 and/or ammonium as nitrogen species are not detectable by voltammetry.

Below the "nitrate suboxic" zone, an "Fe(II)/Fe(III) suboxic" layer (Fig. 3) was observed, and it penetrated to depths of 110 mm at station 8-03 (Fig. 3a) and of 140 mm at station 8-29. Luther et al. (1996) and Taillefert et al. (2000) have shown the potentials of the Fe(III) signals vary depending on aging of Fe(III) solutions and the nature of organic complexes. Generally, the most negative polarographic signal at −0.8 V in the upper part of this layer suggests the presence of "aged" (or strongly bound) Fe(III) complexes. Less negative signals for "fresh" Fe(III) and then the signal for Fe(II) appeared deeper in the sediment revealing very active redox transformations of iron (Fig. 3a,d).

Truly anoxic conditions were found below the "Fe (II)/Fe(III) suboxic" layer (Fig. 3a,e). The reduced sulfur signal (that is either elemental sulfur when Fe(III) was present or sulfide when Fe(III) was absent) was easily detected. The signal for soluble iron monosulfide (Theberge and Luther, 1997) was not found suggesting that reduced Fe is effectively titrated by S to form solid FeS phases including pyrite.

The most unexpected result of voltammetric profiling of these sediments is the absence of Mn(II) that indicates the absence of reactive solid phase manganese in the upper sediment layer. This means that Mn(II), which is easily found in very high concentrations along with Fe (II) in sediments from the suboxic shelf slope (Fig. 5) and which is commonly observed in marine sediments (Gratton et al., 1990; Schaller et al., 1997; Luther et al., 1997, 1998), plays a minor role in sediments from the oxic shelf of the Black Sea, unlike other coastal marine sediments (Canfield et al., 1993; Luther et al., 1999; Van der Zee and Van Raaphorst, 2004). Although we have not analyzed MnOx in these oxic and suboxic sediments yet, dissolved Mn(II) is not observed when MnOx solid phases are low in content as has been shown by Luther et al. (1997) and by Sundby and Silverberg (1981).

3.3. Suboxic sediments (150–300 m water depth)

Sediments from the suboxic part of the shelf slope (station 9-12, Fig. 1) revealed rich manganese and iron but not sulfur chemistry (Figs. 4a and 5). Even the color of the sediment core (Fig. 2b) suggested the presence of Mn(IV) and/or Fe(III). These sediments were brown to grey silt in the upper 50 mm layer of the core and covered with a 10 mm almost black layer of potentially sinking material. The brown layer at a depth of 20–30 mm (Fig. 2b) was much brighter, than the color of clay and silt material from other oxic locations, and it was visually identified as the layer enriched with Mn (IV)–Fe(III) solid phase oxides. Luther et al. (1997) demonstrated that elevated concentrations of dissolved Mn(II) in porewater result from accumulation and reduction of MnO_2 at the oxic/anoxic boundary in the surface layer of sediments. In a laboratory study of a

gravity layer added to the surface of sediments, Chaillou et al. (2007) reported active accumulation of Mn(IV) and Fe(II) solid phases with production of dissolved Mn and Fe. The intensity of the brown color (Fig. 2b) decreased with depth into a fine sandy layer of 50–110 mm. The deeper layers of clay varied slightly in their density and color but revealed rather distinct boundaries easily detected from the voltammetric data (Fig. 4a).

The overall sequence of manganese and iron transformations followed the expected diagenetic changes and redox conditions. Thus, voltammetric profiling showed in the surface layer (Fig. 5a) only the presence of Mn(II) and "aged" Fe(III); MnO_2 was presumably there based on the sediment color. A signal for freshly oxidized Fe(III) appeared deeper and it can be detected at a depth of 40 mm (Fig. 5b) even though the signal of Fe(II) was still not detectable. This layer is where MnO_2 should oxidize all reduced species including Fe(II). The Mn(II) porewater concentration increased with depth to exceed 500 μM at 100 mm, then progressively decreased with depth to remain at a level of 100 μM below 300 mm (Fig. 4a). The signal for Fe(II) appeared at a depth of 60 mm (Fig. 5c) and the signals for Mn(II) and Fe(II) can be easily resolved if the derivative of linear sweep scans is calculated (Fig. 5d). The maximum of about 150 μM porewater concentration of Fe(II) was detected at the depth of 150 mm (Fig. 4a). Deeper in the sediments, the ratio of Fe(II) to Mn(II) increased (Fig. 5e). Both species reached their lowest levels in Layer VI below 300 mm (Fig. 5f). No signals of reduced sulfur or iron monosulfide were detected proving that suboxic sediments rich in Mn (III,IV) and Fe(III) solid phases effectively oxidize organic matter and stopped any flux of reduced sulfur from deeper sediments.

3.4. Sediments from the deep sulfidic part of the sea (Unit I)

Anoxic Unit I sediments are the best known of the Black Sea deposits. They fascinated geochemists of the 1969 ATLANTIS expedition with their fine laminated structure providing a unique opportunity to study sedimentation processes under anoxic conditions over a period of thousands of years (Degens and Ross, 1972). Previous work indicated that Unit I type sediments occur throughout the anoxic part of the Black Sea. Actually, we have recovered such a sediment core (Fig. 2c) from only station 8-7 (Fig. 1). All other sediment cores from the anoxic/sulfidic part of the sea including station 8-30 (Fig. 1) in the center of the western part of the Black Sea contained turbidites.

The vertical structure of Unit I recovered at station 8-07 (Fig. 2C) is precisely as described by Degens and Ross (1972). It was "a microlaminated coccolith ooze" covered with a 10 mm "fluff" layer. The microlaminated structure of the Unit I layer penetrated to a depth of 130–140 mm, where it became indistinguishable from a grey clayish material, which was homogenous in its appearance and extended to the maximum sampled depth of about 600 mm. Only extremely fine grained material was observed after slicing the core for subsamples. Results of preliminary solid phase analyses in the upper 80 mm (Fig. 8a) show reducing characteristics similar to previously published data (Lyons and Berner, 1992; Wijsman et al., 2001b; Anderson and Raiswell, 2004). In the upper 80 mm, pyrite is the dominant solid sulfur phase; dithionite extractable Fe ranges from 7.8 to 14.7 μmol (g dry wt)$^{-1}$ (average = 11.8).

Voltammetric data showed an almost linear increase in the sulfide concentration with depth to a value that is 4-times the maximum concentration of sulfide in the overlying water, which has not been observed in previous studies on Black Sea sediments. Any changes in the structure of sediments at Fig. 2 do not affect this linear growth (Fig. 4b). Though this increase does not reach a maximum within the profiled column, it is expected to reach a maximum in the layer of organic carbon rich Unit II to support reduction of sulfate to sulfide. Published data for the deepest layer of carbon-limited Unit III demonstrate a drop in the concentration of sulfide to non-detectable values (Bezborodov and Eremeev, 1993).

The concentration of sulfide sharply decreased upward within the upper 10 mm "fluff" layer (Fig. 4b). Still, the concentration at the sediment–water boundary remained almost 1.5-times the concentration of sulfide in the overlying waters. These data suggest this site supported a flux of sulfide from sediments to the water column. No other electrochemically active substances, beside sulfide and potentially iron monosulfide (the FeS signal is just above the noise), were detected in porewaters of Unit I from station 8-07.

3.5. Turbidites in deep anoxic cores

Except for station 8-7 (Fig. 1), all other sediment sampling sites in the anoxic part of the Black Sea contained turbidites, rather than Unit I type sediments only, and were wide spread over the sea. This means that the geochemistry of turbidites and exchange processes between turbidites and bottom waters should be of major importance for the water and sediment chemistry of the Black Sea.

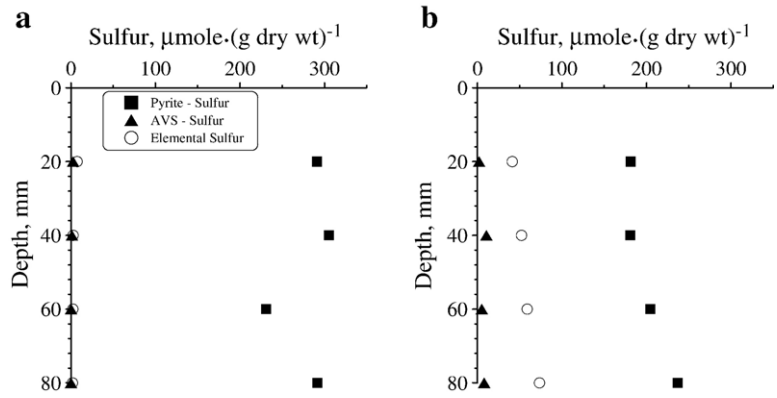

Fig. 8. Solid phase data (sulfur of pyrite — FeS_2, sulfur of acid volatile sulfides — AVS, elemental sulfur — S°) for the cores from stations 8-07 (a) and 8-30 (b).

Turbidites varied from core to core (Fig. 2), even though samples may be obtained from close geographical locations. Wijsman et al. (2001b) also demonstrated extreme spatial variations in the geochemistry of turbidites. Generally, the recovered cores containing turbidites vary in their morphology from a visually homogenous mass to a distinctly multilayer "pie-type" structure. Individual turbidite layers are usually dark grey to almost black and often appear homogenous. Some individual layers may be old "fluff" layers preserved between layers of turbidites but there may also be layers of turbidites of similar or different morphology with concise or diffuse boundaries between individual layers. The vertical structure of sediments is more complex in the western part of the sea, where turbidites have been sampled as far off the shelf slope as the central western station 8-30 (Fig. 1). Their lithology varies from clay through silt to fine grained sand. These variations in their morphology and lithology clearly demonstrate that turbidites vary in their origin. They may originate from the shelf, shelf-edge or slope areas (Wijsman et al., 2001b) and from multiple events with different energy and dynamics.

The dramatic variations in the appearance of deep anoxic cores other than station 8-07 suggest rich porewater chemistry and the results of voltammetric profiling (Fig. 6) confirm this. Voltammetric data showed all three possible profiles for sulfide: decreasing (Fig. 6b), increasing (Fig. 6f), and unchanged (Fig. 6d) concentrations with depth. The sulfide profiles can be smooth or show deviations with depth but the major features are reproduced in duplicate profiles (e.g.; Fig. 6a, d, e). The boundaries between individual layers of turbidites are usually characterized by abrupt changes in the concentration or changes in the type of the vertical distribution of the traced redox species (e.g., Fig. 6a, c).

The concentration of sulfide usually declined from the upper part of the core to its deeper layers. This is true for all other deep anoxic cores with turbidites from the 2003 KNORR and 2005 ENDEAVOR expeditions that are not presented in this work. The drop in concentration varied from site to site [e.g., stations 8-19 (Fig. 6a) and 8-30 (Fig. 6e)] and could result in almost complete disappearance of sulfide as in station 9-06 (Fig. 6b). Turbidites at station 9-05 (near where the slope meets the abyssal plain) from the south-western part of the sea revealed the most complex multi-layer vertical structure and also the most irregular vertical profiles of sulfide in porewater (Fig. 6c) as neighboring sediment layers in the core showed sulfide increases and decreases.

Cores taken from along the slope in the upper anoxic waters (330 water depth) had higher sulfide concentrations than those from the abyssal plain (station 9-08, Fig. 6f). The highest concentration of sulfide in these sediments was about 600 µM which exceeds by about 200 µM the highest concentration of sulfide in the deep Black sea water column and is as much as 6 times the concentration of sulfide in overlying waters along the slope. These data demonstrate the flux of sulfide from the sediments to the overlying water column as predicted by Vainshteyn et al. (1986).

In addition to sulfide, one other voltammetric signal at −1.2 V (Fig. 9) was detected in porewaters from anoxic zone cores with turbidites. This signal is due to soluble iron monosulfide (FeS_{aq}). It cannot be used to calculate concentrations (Theberge and Luther, 1997) as there is no standard for this material at present, but the higher the intensity of this signal the higher the content of FeS_{aq}. Preliminary solid phase analyses (Fig. 8b) of the upper 80 mm confirm the concentration of AVS is higher in cores with turbidites by an average of five fold as compared to AVS found in Unit I (Fig. 8a). More

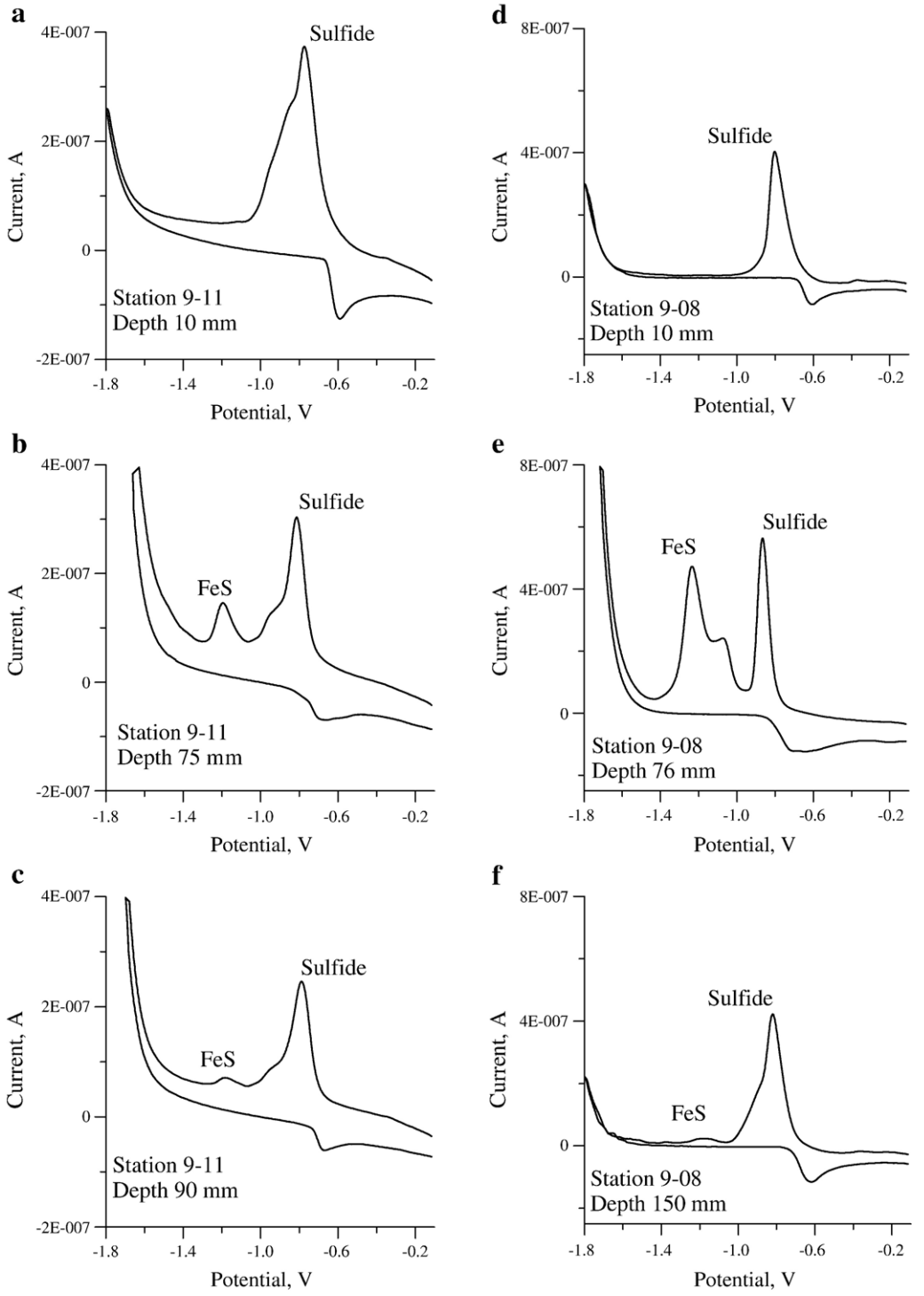

Fig. 9. Individual voltammetric linear cyclic scans at specific depths of the anoxic sediment core containing turbidites at station 9-11 (a–c) and at station 9-08 (d–f).

importantly elemental S approaches one-half the pyrite value (Fig. 8b). Dithionite extractable Fe ranges from 98.4 to 138.4 μmol (g dry wt)$^{-1}$ (average = 122.0) and is higher by an average of 110 μmol (g dry wt)$^{-1}$ than station 8-07 (Unit 1). Thus, these cores are more oxidized, and geochemical properties vary in cores with

turbidites, as has been previously published by Wijsman et al. (2001b).

The major conclusion concerning deep anoxic zone cores is that turbidites are far more abundant in the Black Sea than previously assumed, and that they vary dramatically in both their morphology and chemistry.

4. Discussion

4.1. Oxic sediments

Sediments from the oxic shelf area of the Black Sea are similar in many ways to sediments from other aerobic marine systems, though there is one important difference. The sequence of oxidants governing redox geochemical processes include oxygen, nitrate, MnO_2, Fe(III) oxides, and sulfate (Luther et al., 1997; Anschutz et al., 2000). The depth of O_2 penetration in the Black Sea shelf oxic sediments (Fig. 3) is typical for coastal and other nearshore marine environments, where it is limited to the upper 10 mm (Luther et al., 1997, 1998; Taillefert et al., 2000; Hyacinthe et al., 2001). Below the oxic layer, nitrate is the next major oxidizer. Though nitrate is not detectable with the Au/Hg electrode, the absence of any other voltammetric signals is an indicator of nitrogen redox transformations in this layer. Between the layers of nitrogen and sulfur redox transformations, Fe(III)–Fe(II) and Mn(IV)–Mn(II) reactions are expected (Postma, 1990; Postma and Jakobsen, 1996) but only those for Fe(III)–Fe(II) have been detected (Fig. 3). The analytical limit for voltammetric Mn(II) and Fe(II) detection is close to 5 μM and 15 μM respectively (Brendel and Luther, 1995; Luther et al., 1998). Fe(II) was easily detected in sediments from the oxic part of the sea (Fig. 3) and both Mn(II) and Fe(II) are detected in sediments from the suboxic zone (Fig. 5). Wijsmana et al. (2002) reported that the maximum concentration of Mn(II) in porewaters of the north-western Black Sea sediments was 10 to 15 μM which would be detected by voltammetry.

One explanation of the lack of Mn(II) in our cores from the oxic part of the sea is related to local sources of manganese and iron. The major sources of these metals for the Black Sea are rivers and atmospheric deposition (Mitropolsky et al., 1982). Thamdrup et al. (2000) and Wijsmana et al. (2002) published data for the north-western Black Sea (location C in Fig. 1). This area forms an underwater canyon from the Danube River to the deep part of the sea. This canyon may collect a major part of the manganese delivered with the river waters to the sea as shown in the St. Lawrence estuary by Sundby and Silverberg (1981). We may expect a significant flux of iron but not manganese from sediments in the area of Kerch peninsular in the eastern part of Crimea because this is an area of active iron ore mining (Mitropolsky et al., 1982). Another similar mining region is located in the Anatolian mountains bordering the south-eastern part of the sea (Duman et al., 2006). Thus, the lack of manganese in sediments from the oxic shelf south from Crimea (station 8-03, Fig. 1) and north of the Anatolian coast (station 8-29, Fig. 1) is likely due to smaller inputs of terrestrial manganese relative to iron.

Another explanation for the patchiness of the manganese content in sediments from the oxic part of the sea could be related to the presence of oxic, suboxic, and anoxic water column zones in the Black Sea, which are vertically separated. Manganese is diagenetically reduced in sediments supporting its flux from deeper to upper layers of sediments and to the water column. It is oxidized in the upper layers of sediments or in oxic waters to precipitate back to sediments (Fig. 10a). If the entire area of the sea is oxic, redox transformations and physical processes result in redistribution of manganese from its initial sources across the bottom (Sundby and Silverberg, 1981) and in accumulation of MnO_2 in the upper sediments (Luther et al., 1997). Anoxic conditions support accumulation of dissolved Mn(II) whereas oxic sediments become depleted in manganese. A similar process has been suggested to explain relative depletion of reactive iron in sediments from the oxic area of the Black Sea and its accumulation in sediments under sulfidic waters (Wijsman et al., 2001a; Anderson and Raiswell, 2004). This mechanism of Mn depletion of sediments from the oxic part of the Black Sea should be more effective for manganese because it is reduced more readily than iron.

The major difference between accumulation of manganese and iron is that dissolved Mn(II) is accumulated in the anoxic water column, while iron sulfide and pyrite is accumulated in sediments of the anoxic part of the sea. The vertical profile of Mn(II) in the oxic–anoxic water column of the Black Sea (Lewis and Landing, 1991; Konovalov et al., 2004) suggests its upward flux from the anoxic zone and its effective oxidation to Mn(IV) in the suboxic zone. The suboxic zone basically serves as a trap preventing transport of Mn(II) to oxic waters (Fig. 10a). Available data suggest that the water column profile and the upward flux of Mn(II) always expire in the suboxic zone. The flux of sinking Mn(IV) from the suboxic zone results in precipitation and reductive dissolution of Mn(IV) in the upper anoxic layers of the water column, where a local maximum of Mn(II) is detected (Lewis and Landing, 1991; Konovalov et al., 2004). A part of

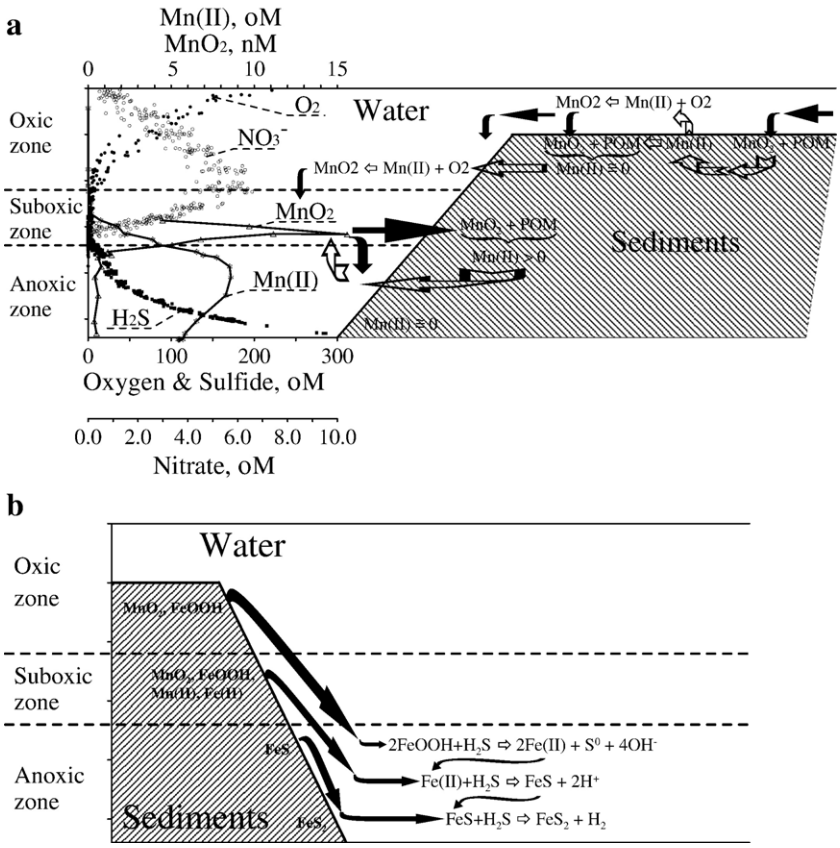

Fig. 10. (a) Scheme of manganese cycling in the Black Sea waters and sediments; the concentrations of the chemical species plotted are from Konovalov and Murray (2001) with Mn data from Lewis and Landing (1991). Precipitation of MnO_2 to oxic sediments is compensated by digenetic remobilization of Mn(II) from these sediments. The maximum flux of MnO_2 occurs in the suboxic zone and near the coast. It maintains the highest concentration of manganese in these sediments. (b) zones from which turbidites containing different redox species originate and are transported to deep anoxic sediments. The equations indicate possible Fe reactions when materials from these zones reach the anoxic deep waters and sediments. Not shown on the figure is the reaction of MnO_2 from suboxic zone sediments which can oxidize H_2S to S_8.

sinking Mn(IV) may also reprecipitate at the shelf slope suboxic zone to support its inventory in sediments (Fig. 4a). We cannot rule out an upward flux of Mn(II) due to upwelling at the periphery of the deep part of the sea. This would result in more intensive production of MnO_2 that leads to a higher flux of MnO_2 to the shelf slope sediments. This fits our data on higher concentrations of manganese in the suboxic sediments and it also fits data on higher concentrations of MnO_2 near the shelf slope (Murray et al., 2003), but more data are needed to quantify the effect of upwelling for the manganese budget.

4.2. Suboxic sediments

Voltammetric data showed that Mn(II) and Fe(II) are the only soluble redox species throughout the 350 mm sediment core from the suboxic part of the Black Sea (Station 9-12, Figs. 1, 4a and 5), except for the potential contribution of nitrogen in the upper part of the sediment core. Oxygen and reduced sulfur species were not observed, thus these sediments are anoxic but non-sulfidic. The concentration of manganese (II), which exceeds 100 μM at the sediment–water boundary (Fig. 4a), should provide very fast and effective consumption of oxygen, if any is available. Nitrate can potentially exist in the upper 30 mm sediment layer, where Mn(II) and "aged" Fe(III) are the only electrochemically active species. Unlike manganese (II), iron (II) is readily oxidized by nitrate (Postma, 1990; Ottley et al., 1997) and by Mn(IV) (Postma and Appelo, 2000); thus, the absence of dissolved iron (II) in the upper 30 mm is likely. "Aged" Fe(III) was observed via the broad irreversible signal at −0.8 V (Fig. 5a). Taillefert et al. (2000) showed this signal is formed on aging Fe(III) solutions. Freshly oxidized Fe(III) becomes

detectable at the depth of 40 mm (Fig. 5b) suggesting that this is a boundary between nitrate and iron dominated layers. The rest of the core from 60 mm to the maximum profiled depth of 350 mm showed Mn(II), Fe(II), and Fe(III) suggesting that the redox chemistry is dominated by manganese and iron transformations. Fe(II) becomes measurable at 50 mm so the production of Mn(II) appears partially related to the reaction of Fe(II) with MnO_2 but most reduction of MnO_2 is due to organic matter decomposition, as the concentrations of Fe(II) are not enough to support the observed level of reduction of MnO_2 to Mn(II). Indeed, the detected maximum of about 150 μM of Fe(II) can support reduction of about 75 μM of MnO_2 to Mn(II). Thus, more than 400 μM of Mn(II) must be produced due to diagenetic reduction of MnO_2 by organic matter. Manganese and iron oxides likely balance the reducing potential of organic matter, as has been reported for other systems (Canfield et al., 1993; Van der Zee and Van Raaphorst, 2004), and prevent sulfate reduction in the lower part of the core. Thus, these sediments are an example of a classic sequence of redox species governing processes between oxic and sulfidic conditions.

The porewater profile of dissolved Mn(II) showed a maximum at a depth of 100 mm (Fig. 4a) suggesting an upward flux of Mn(II) above the depth of 100 mm and a downward flux into deeper sediments (Fig. 7b). The reconstructed profile of the vertical flux of Mn(II) (Fig. 7b) shows that the upward flux varies in its magnitude but generally increases to reach the maximum value of ~400 mM m^{-2} yr^{-1} at the sediment–water boundary. The observed range of concentrations (Fig. 4a) and upward fluxes (Fig. 7b) are similar to those reported in the laboratory by Chaillou et al. (2007).

The concentration of Mn(II) below its maximum decreased almost linearly with depth in layer IV from 110 to 250 mm and the downward flux is almost constant in this layer (Fig. 7b), but the profile becomes convex in layer V from 250 to 300 mm (Fig. 4a). This suggests that the distribution of dissolved Mn(II) is mainly governed by its diffusion in layer IV, but some manganese consumption, for example precipitation of manganese carbonates, is likely in layer V. The downward flux below the maximum of Mn(II) reaches its maximum value of ~35 mM m^{-2} yr^{-1} in layer V. We assume that processes are close to a steady state in layer VI.

The presence of upward and downward fluxes (Fig. 7b) of Mn(II) above and below the maximum of the porewater concentration (Fig. 4a) suggests that the source of manganese is confined to the upper sediments, rather than to any deep sedimentary sources. While deep layers of sediments could serve as a source of manganese, an external permanent flux of manganese should exist in the Black Sea to maintain the profile of dissolved Mn(II) at a steady state on the time scale of centuries to millennia. The only feasible source of manganese for these sediments is the flux of sinking MnO_2 from the suboxic zone bordering the Black Sea shelf slope.

We propose that the vertical separation of oxic, suboxic and anoxic water column zones in the Black Sea creates an effective Mn sedimentary cycle (Fig. 10a) that can help control the Mn(II) distribution in both sediments and water. Similar to iron (Wijsman et al., 2001a; Anderson and Raiswell, 2004), manganese is diagenetically remobilized in shelf sediments from the oxic part of the sea via successive reduction of Mn(III, IV) oxides and oxidation of Mn(II). Physical processes then push fine grained material containing Mn(III, IV) oxides from the shelf to the shelf edge (Sundby and Silverberg, 1981) where suspended Mn(III, IV) oxides are pushed out into the water column and either redeposit on suboxic sediments or reach the suboxic and anoxic waters where sulfide reduces them to Mn(II). The Mn(III,IV) oxides that settle on suboxic sediments are reduced during organic matter decomposition, which explains the high concentrations of Mn(II) found in porewaters from the suboxic zone. Some of this dissolved Mn(II) fluxes into the overlying waters and along with the upward flux of dissolved Mn(II) from the anoxic waters can be reoxidized in the water column of the suboxic zone to reform Mn(III, IV) oxides, which settle onto the suboxic zone sediments or are reduced again in the anoxic water column as they sink.

The suboxic sediments of the Black Sea serve as a source of dissolved Mn(II) to the water column (Fig. 7), but this source of manganese is partially offset by MnO_2 precipitation from the water column to the sediments. The major part (~92%) of the flux of MnO_2 to the suboxic sediments is diagenetically reduced to support its upward flux of Mn(II), while the remaining part is preserved in sediments. This recycling of Mn supports accumulation of manganese in suboxic shelf-slope sediments, which are a net sink of manganese on a basin-wide scale.

4.3. Deep anoxic sediments (Unit I) without turbidites

Published solid-phase data for deep sulfidic cores suggest only a Unit I structure in the upper 200 to 500 mm layer, which is spatially uniform on a basin-wide scale (Degens and Ross, 1972; Lyons and Berner,

1992). Thus the porewater chemistry should also be spatially uniform and vertically predictable. Sulfide, for example, should increase with depth approaching organic carbon rich Unit II (organic carbon rich sapropel), then it should decrease within carbon-limited Unit III (Bezborodov and Eremeev, 1993). Iron in Unit I is expected mainly as pyrite (>80% of the total iron content) and some iron monosulfide that is a transient product of pyritization (Lyons, 1997). Mn(II) could potentially co-precipitate with pyrite (Huerta-Diaz and Morse, 1992).

Our results of voltammetric profiling of the core of microlaminated Unit I at station 8-07 (Fig. 1) demonstrate that iron monosulfide as FeS_{aq} (Theberge and Luther, 1997), Mn(II) and Fe(II) are below their detection limits. No other forms of reduced sulfur other than sulfide were detected. This agrees with the previously published data by Lyons (1997). Still, the sulfide concentration dramatically increases within and below the "fluff" layer reaching ~1200 μM at the depth of 10 mm and ~1600 μM at the maximum profiled depth. The vertical gradient of the concentration of sulfide is almost constant revealing no limits to the growth of sulfide and suggesting only an upward diffusion in this layer from some source of sulfide below the profiled depth (Fig. 4b), which is presumably the layer of organic-rich Unit II. Though an increase in the concentration of sulfide is expected based on previous reports by Bezborodov and Eremeev (1993) and by Lyons and Berner (1992), the range of the increase is impressive. The highest previously reported concentration of ~700 μM for Unit I at the central station south of Crimea (location B in Fig. 1) is almost twice as much as the 400 μM in the bottom waters (Lyons and Berner, 1992). But this value is twice as low as the observed concentration of ~1600 μM at our central eastern station 8-7 (Figs. 1 and 4b). The 3-fold increase in the upper 10 mm (Fig. 4b) supports the flux of sulfide from sediments to the overlying water column.

When our data (Fig. 4b) for all deep cores are compared with each other and to those published by Lyons and Berner (1992), the porewater chemistry of Unit I appears to be spatially not so uniform. The vertical profile of sulfide varies dramatically over the basin but shows a very consistent spatial tendency. It is 55% of the sulfide level in the overlying bottom waters in the western part (Fig. 6e), almost 2-fold greater than the bottom waters in the central part (Lyons and Berner, 1992), and 4-fold greater than what we observed in the eastern part (Fig. 4b). As the organic carbon distribution in Unit I does not support large spatial variations in sulfide and organic carbon rich Unit II is also expected to provide a spatially uniform source of sulfide, other processes must occur. The high levels and the linear profile of sulfide in Unit I (Fig. 4b) are indicative of an intensive production of sulfide in sapropel layers of Unit II. The fact that the eastern euxinic sediments support an upward flux, while the western euxinic sediments consume sulfide, is beyond doubt. The latter is likely due to sulfide oxidation when suboxic sediments rich in MnO_2 and Fe(III) solid phases slump into the deep basin (see below).

Regardless of the shape of the sulfide profile in sediments, the "fluff" layer always reveals higher concentrations of sulfide, as compared to the overlying waters. Albert et al. (1995) reported the rate of sulfate reduction in the "fluff" layer is 10 times higher than for deeper sediments. This suggests that the "fluff" layer, when it overlays sediments, is the source of sulfide for the water column. The magnitude of this source should depend on the flux and quality of organic matter, the rate of its respiration, and on the magnitude and direction of the flux of sulfide in underlying layers of sediments. Still, this flux can be either increased by an additional flux of sulfide from deeper layers of sediments, as in the central eastern part (station 8-07, Fig. 4b), or partially consumed by deeper sediments, as found in the central western part of the Black Sea (station 8-30, Fig. 6e).

4.4. Deep anoxic sediments with turbidites

The major part of the upper anoxic sediments contained turbidites, which have been found over the anoxic part of the shelf slope and even at the abyssal plain. Canfield et al. (1996) have also reported that turbidites have been found throughout the central and southern part of the sea. Though Lyons and Berner (1992) reported Unit I type sediments at their central western station in 1988 (near our station 8-30), we have now found turbidites at station 8-30, as well as at stations 8-19, 8-23, 9-05, 9-06 and E-07 (Fig. 1). This potentially means that turbidite deposition has become more active in recent years, most probably due to the two destructive earthquakes in 1999 in NW Turkey. Indeed, this region is a site of dense tectonic activity, a detailed account of which is given in Şengör et al. (2005). In any case, it appears that water–sediment exchange processes are now mainly influenced by turbidites in most of the Black Sea. Variations in porewater sulfide profiles are dominated by variations in turbidite composition and deposition (Fig. 6).

The cores showed that turbidites (Fig. 2) could reach to the deepest layers sampled. They can also overlay

Unit I, or previously deposited turbidites, and they can even interlay and safely trap old "fluff" layers. Our observations are consistent with some previously published data on turbidites (Lyons and Berner, 1992; Arthur et al., 1994). However, the cores sampled also show that variations in the vertical sulfide profiles and the number of turbidite layers are more complex where the slope in the southwest meets the abyssal plain (e.g., Fig. 6c) and less complex toward the west center of the Black Sea (Fig. 6e).

The individual turbidite layers found in 2003 do not always appear homogenous. Similar data have been published by Hurtgen et al. (1999) although Arthur et al. (1994) have reported that turbidites can be "extremely homogenous in color, grain size (<2μm), and chemistry". Data published by Arthur et al. (1994), by Lyons and Berner (1992), and recently by Lyons and Kashgarian (2005) suggest that turbidites can have "nearly identical C–S chemistries", even though the samples were taken from widely spaced locations. However, Wijsman et al. (2001a) have reported on substantial variations in AVS and pyrite contents and sulfur isotope composition between cores with turbidites taken a short distance apart. Wilkin and Arthur (2001) also reported on vertical changes in $\delta^{34}S$ values. Our data demonstrate that turbidites can be of different colors from grey to black and may vary in morphology from fine grained sand to silt and further to clayish mud, similar to that reported by Hurtgen et al. (1999).

The fact that there are spatial variations in the number of individual layers, their thickness, color and morphology suggest that turbidites originate from a number of sites in multiple events of different intensities. Different turbidites can occasionally reveal similar geochemical properties (Lyons and Kashgarian, 2005), but this should not be a general rule for all turbidites in the Black Sea. Our voltammetric data in Fig. 6 clearly demonstrate an extreme variety in porewater chemistry.

The origin of turbidites is generally considered to be from the shelf and slope areas (Wijsman et al., 2001b), but the original sediments, which form turbidites, can be expected to have a wide variety of chemical properties (Fig. 10b). For example, sediments formed under oxic waters possess Fe(III)oxyhydroxides and potentially nitrate (Fig. 3). In contrast the slope sediments can form under (i) suboxic conditions and contain Mn(II), Mn(III, IV) oxides and Fe(III)oxyhydroxides (Figs. 4a and 5) or (ii) anoxic conditions and contain sulfide (Fig. 6f). Lateral injections of material from the upper parts of the shelf and/or slope to deeper sediments may change the sulfide profile by decreasing the sulfide concentration (Fig. 6a,e). Sulfide can be completely consumed, if the re-deposited turbidites are rich in MnO_2, Fe(II) or FeS. Thus, sulfide is usually depleted in turbidites at the base of slope (Fig. 6a,b) and even on the euxinic plain (Fig. 6e).

Sediment–water exchange processes and processes during re-deposition of turbidites may even affect bottom water chemistry. Thus, data from the 2003 KNORR cruise revealed a reproducible sulfide decrease by about 30 μM in the 20 m overlying bottom water (Fig. 11). This change in the vertical distribution of sulfide has never been reported for the bottom homogeneous water column layer as all vertical distributions are expected to be uniform in this layer and any detectable changes are expected on a time scale of decades to centuries (Murray et al., 1991; Konovalov and Murray, 2001). The concentration of sulfide decreases by another 150 μM in the upper 120 mm of sediments at station 8-30 (Fig. 6e) and sulfide decreases to almost complete disappearance below 160 mm at station 9-06 (Fig. 6b). The best possible explanation is that earthquakes triggered massive deposition of oxidized sediments to these areas. Oxidized sediment that possesses only 1 μmol cm^{-3} of FeOOH (this value is extremely low, as the usually reported concentrations of reactive Fe in sediments are tens to hundreds times higher, e.g. Wijsman et al., 2001a,b; see above) can support diagenetic consumption during pyritization of over 2500 μM of sulfide when it slides into the deeper sediments (equations in Fig. 10b). The latter value is about 6 times higher than the total concentration of sulfide in Black Sea bottom waters.

In addition to a wide range of initial geochemical properties, sediments that result in turbidites become unstable in different areas at different times depending on the scale of an event that dislodges them. A turbid flow can propagate >700 km in the Atlantic Ocean

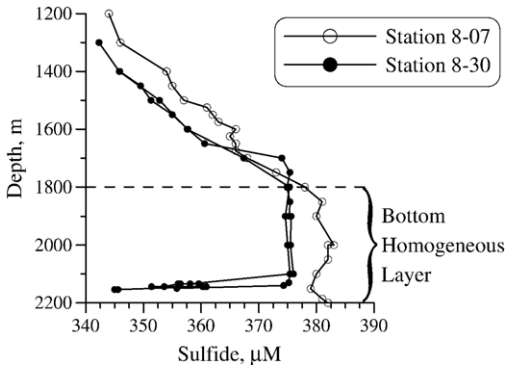

Fig. 11. The vertical profiles of sulfide at eastern central station 8-07 and at western central station 8-30 (two profiles from independent casts).

(Dade and Huppert, 1994), so a turbidite flow may potentially cover the distance of 100–200 km reaching the central part of the Black Sea. If the starting impulse is strong such as earthquakes, the initial flow will include particles of different sizes. The flow can propagate rapidly down the slope and can destroy and/or entrain the crossed sediments. This event cannot be low energy at its initial stage. When a turbid flow propagates towards the euxinic plane, the energy decreases and causes size fractionation of the initial material, as the flow collapses under its weight. This results in vertical and spatial variations in re-deposited turbidites. Only the fine fraction of initial sediments in a low energy process may reach the areas of the euxinic plane far from the slope. These turbidites can form the layers that do not result in any damage to the underlying sediments (Arthur et al., 1994). Fractionation of initial sediments results in a variety of solid-phase and porewater properties of re-deposited turbidites along the route of the turbid flow. Variations in the energy of initial events and in the composition of initial sediments (Fig. 10b) explain and support the observed complexity in the sulfide porewater profiles observed in Fig. 6c. Unlike the central part of the sea, the area where the base of the slope meets the abyssal plain is accessible by the majority of turbidite flows.

Generally, when the vertical structure of turbidites is more complex and the profile of sulfide is less regular, the dissolved iron monosulfide, FeS_{aq}, voltammetric signal is found (Fig. 9). A higher current for the FeS_{aq} signal is usually found at the boundaries of individual layers of turbidites likely due to new Fe(III) input and its reduction by sulfide (equations in Fig. 10b). Iron monosulfide species are a kinetically controlled intermediate product of iron pyritization (Richard, 1997; Rickard and Luther, 1997). FeS is produced faster than pyrite and must react with zerovalent sulfur or H_2S to form FeS_2. When an additional source of Fe(III) becomes available in sulfidic sediments, the Fe(III) must react with H_2S to form Fe(II) which in turn reacts further with H_2S to form FeS phases. If all the H_2S is consumed, then FeS_{aq} exists as an intermediate product and is evidence of disturbance in sediments.

Thus, the composition of turbidites is a function of the composition of the original sediments, the scale of the turbidites flow, the presence and topography of canyons, the distance from their area of their origin, their composition at the moment of their re-deposition, and finally the time passed after the event of re-deposition. We believe our data provides a partial explanation of the statement by Lyons (1997) that the composition of turbidites suggests "…a complicated depositional/diagenetic scenario of nonsteady-state behavior". Future studies should address the kinetics of diagenetic processes in sediments and the importance of water–sediment exchange processes for the overall budget of geochemical species and elements in the Black Sea.

5. Conclusions

Voltammetric profiling was performed on the upper layer of the Black Sea's sediments obtained from the oxic, suboxic, and sulfidic parts of the water column. Sediments from the oxic part of the sea, though spatially variable in their morphology and lithology, showed similar porewater chemistry. The sequence of redox processes and constituents is typical for coastal and other nearshore marine environments, except for the lack of detectable manganese (II). Remobilization of manganese from these sediments leads to dissolved Mn accumulation in the anoxic waters and in suboxic sediments.

Porewaters from the suboxic sediments are unlike those from the oxic zone as they are enriched in Mn(II), Fe(II) and their oxides. Reduced sulfur was not detected to the maximum profiled depth of 350 mm suggesting that manganese and iron redox transformations effectively control mineralization of organic carbon and prevent any flux of sulfide from the deeper sediment layers. The concentrations, which can reach 500 μM for Mn(II) and 100 μM for Fe(II), are higher than that found in the water column [6–8 μM of Mn(II) and 200–300 nM of Fe(II)]. This difference suggests that suboxic zone sediments are the source of dissolved manganese and iron for the water column. The vertical profiles of Mn(II) show both an upward and downward flux of Mn (II) indicating precipitation of oxidized Mn from the water column and its diagenetic accumulation in sediments. Most of the dissolved manganese is diagenetically recycled in sediments and into the water column. About 8% of the dissolved manganese in suboxic sediments is accumulated in deeper layers of sediments. While iron is effectively accumulated in the form of pyrite in deep anoxic sediments, sediments of the suboxic zone are a net sink of manganese on the basin-wide scale.

The distribution of sulfide in anoxic cores varied dramatically and increased in concentration from the western to the eastern part of the sea. The concentration of sulfide in sediments of the central western station was only 55% of its maximum value in the bottom waters and it decreased with depth, but it was 4 times the bottom water value at the eastern central station. Sulfide concentrations also increased in the overlying bottom

waters from the western central to the eastern central basin. These variations in sulfide levels indicate that sulfide oxidation and pyritization dominate in the western part of the sea, due to the input of turbidites enriched in manganese and iron oxides, whereas pyritization is the dominant reaction in the eastern part.

Our data suggest that anoxic Unit I type sediments without turbidites are limited to the very central part of the sea, while anoxic sediments with turbidites are found at the slope, where the slope meets the abyssal plain and over the western part of the abyssal plain. Recent earthquakes apparently resulted in massive displacement of sediments from the shelf and slope areas of NW Turkey generating turbidites that propagate to the central western part of the sea. These turbidites have resulted in massive consumption of sulfide both within the sediments and even in the bottom anoxic waters.

Acknowledgements

This work was supported by CRDF grant # UKG2-2645-SE-05. The authors also acknowledge NSF grant OCE-0096365 that made possible the 2003 KNORR and 2005 ENDEAVOR expeditions to the Black Sea. Results on the vertical distribution of sulfide in the Black Sea water column were provided by A.S. Romanov from Marine Hydrophysical Institute, Ukraine. The paper substantially benefited from comments by Jack Middelburg and two other anonymous reviewers.

References

Albert, D.B., Taylor, G., Martens, C., 1995. Sulfate reduction rates and low molecular weight fatty acid concentrations in the water column and surficial sediments of the Black Sea. Deep-Sea Research 42, 1239–1260.

Anderson, T.F., Raiswell, R., 2004. Sources and mechanisms for the enrichment of highly reactive iron in euxinic Black Sea sediments. American Journal of Science 304, 203–233.

Anschutz, P., Sundby, B., Lefrançois, L., Luther III, G.W., Mucci, A., 2000. Interactions between metal oxides and species of nitrogen and iodine in bioturbated marine sediments. Geochimica et Cosmochimica Acta 64, 2751–2763.

Arthur, M.A., Dean, W.E., Neff, E.D., Hay, B.J., King, J., Jones, G., 1994. Varve calibrated records of carbonate over the last 2000 years in the Black Sea. Global Biogeochemical Cycles 8, 195–217.

Berner, R.A., 1974. Iron sulfides in Pleistocene deep Black Sea sediments and their paleo-oceanographic significance. In: Degens, E.T., Ross, D.A. (Eds.), Black Sea-Geology, Chemistry, and Biology. Am. Assoc. Pet. Geol. Mem., vol. 20, pp. 524–531.

Bezborodov, A.A., Eremeev, V.N., 1993. Chernoe more. Zona vzaimodeistviya aerobnikh I anaerobnikh vod (The Black Sea. The Layer of Interaction of Aerobic and Anaerobic Waters). MHI, Sevastopol. 299 pp. (in Russian).

Brendel, P.J., Luther III, G.W., 1995. Development of a gold amalgam voltammetric microelectrode for the determination of dissolved Fe, Mn, O2, and S(−II) in porewaters of marine and freshwater sediments. Environmental Science and Technology 29, 751–761.

Bull, D.C., Taillefert, M., 2001. Seasonal and topographic variations in porewaters of a southeastern USA salt marsh as revealed by voltammetric profiling. Geochemical Transactions 13.

Calvert, S.E., Karlin, R.E., 1991. Relationships between sulphur, organic carbon, and iron in the modern sediments of the Black Sea. Geochimica et Cosmochimica Acta 55, 2483–2490.

Canfield, D.E., Jørgensen, B.B., Fossing, H., Glud, R., Gundersen, J., Ramsing, N.B., Thamdrup, B., Hansen, J.W., Nielsen, L.P., Hall, P.O.J., 1993. Pathways of organic carbon oxidation in three continental margin sediments. Marine Geology 113, 27–40.

Canfield, D.E., Lyons, T.W., Raiswell, R., 1996. A model for iron deposition to euxinic Black Sea sediments. American Journal of Science 296, 818–834.

Chaillou, G., Anschutz, P., Dubrulle, C., Lecroart, P., 2007. Transient states in diagenesis following the deposition of a gravity layer: dynamics of O_2, Mn, Fe and N-species in experimental units. Aquatic Geochemistry 13, 157–172.

CIESM, 2002. Turbidite systems and deep-see fans of the Mediterranean and the Black Seas. CIESM Workshop Series, vol. 17. Monaco.

Dade, W.B., Huppert, H.E., 1994. Predicting the geometry of chanellized deep-sea turbidites. Geology 22, 645–648.

Degens, E.T., Ross, D.A., 1972. Chronology of the Black Sea over the last 25,000 years. Chemical Geology 10, 1–16.

Duman, M., Duman, Ş., Lyons, T.W., Avcı, M., İzdar, E., Demirkurt, E., 2006. Geochemistry and sedimentology of shelf and upper slope sediments of the south-central Black Sea. Marine Geology 227, 51–65.

Glazer, B.T., Luther III, G.W., Konovalov, S.K., Friederich, G.E., Trouwborst, R.E., Romanov, A.S., 2006. Spatial and temporal variability of the Black Sea suboxic zone. Deep-Sea Research. II 53, 1756–1768.

Gratton, Y., Edenborn, H.M., Silverberg, N., Sundby, B., 1990. A mathematical model for manganese diagenesis in bioturbated sediments. American Journal of Science 290, 246–262.

Huerta-Diaz, M.A., Morse, J.W., 1992. The pyritization of trace metals in anoxic marine sediments. Geochimica et Cosmochimica Acta 56, 2681–2702.

Hurtgen, M.T., Lyons, T.W., Ingall, E.D., Cruse, A.M., 1999. Anomalous enrichments of iron monosulfide in euxinic marine sediments and the role of H_2S in iron sulfide transformations: examples from Effingham inlet, Orca Basin, and the Black Sea. American Journal of Science 299, 556–588.

Hyacinthe, C., Anschutz, P., Carbonel, P., Jouanneau, J.-M., Jorissen, F.J., 2001. Early diagenetic processes in the muddy sediments of the Bay of Biscay. Marine Geology 177, 111–128.

Konovalov, S.K., Murray, J.W., 2001. Variations in the chemistry of the Black sea on a time scale of decades (1960–1995). Journal of Marine Systems 31 (1–3), 217–243.

Konovalov, S.K., Luther III, G.W., Friederich, G.E., Nuzzio, D.B., Tebo, B.M., Murray, J.W., Oguz, T., Glazer, B., Trouwborst, R.E., Clement, B., Murray, K.J., Romanov, A.S., 2003. Lateral injection of oxygen with the Bosporus plume-fingers of oxidizing potential in the Black Sea. Limnology and Oceanography 48, 2369–2376.

Konovalov, S., Samodurov, A., Oguz, T., Ivanov, L., 2004. Parameterization of iron and manganese cycling in the Black Sea suboxic and anoxic environment. Deep-Sea Research. I 51, 2027–2045.

Lewis, B.L., Landing, W.M., 1991. The biogeochemistry of manganese and iron in the Black Sea. Deep-Sea Research 38 (Suppl. 2A), S773–S804.

Luther III, G.W., Shellenbarger, P.A., Brendel, P.J., 1996. Dissolved organic Fe(III) and Fe(II) complexes in salt marsh porewaters. Geochimica et Cosmochimica Acta 60 (6), 951–960.

Luther III, G.W., Sundby, B., Lewis, B.L., Brendel, P.J., Silverberg, N., 1997. Interactions of manganese with the nitrogen cycle: alternative pathways to dinitrogen. Geochimica et Cosmochimica Acta 61 (19), 4043–4052.

Luther III, G.W., Brendel, P.J., Lewis, B.L., Sundby, B., Lefrançois, L., Silverberg, N., Nuzzio, D.B., 1998. Simultaneous measurement of O_2, Mn, Fe, I^-, and S(−II) in marine pore waters with a solid-state voltammetric microelectrode. Limnology and Oceanography 43 (2), 325–333.

Luther III, G.W., Reimers, C.E., Nuzzio, D.B., Lovalvo, D., 1999. In situ deployment of voltammetric, potentiometric, and amperometric microelectrodes from a ROV to determine dissolved O_2, Mn, Fe, S(−2), and pH in porewaters. Environmental Science & Technology 33, 4352–4356.

Luther III, G.W., Glazer, B.T., Hohmann, L., Popp, J.I., Taillefert, M., Rozan, T.F., Brendel, P.J., Theberge, S.M., Nuzzio, D.B., 2001. Sulfur speciation monitored in situ with solid state gold amalgam voltammetric microelectrodes: polysulfide as a special case in sediments, microbial mats and hydrothermal vent waters. Journal of Environmental Monitoring 3, 61–66.

Luther, III G.W., Glazer, B.T., Ma, S., Trouwborst, R.E., Moore, T.S., Metzger, E., Kraiya, C., Waite, T.J., Druschel, G., Sundby, B., Taillefert, M., Nuzzio, D.B., Shank, T.M., Lewis, B.L., Brendel, P.J., in press. Use of voltammetric solid-state (micro)electrodes for studying biogeochemical processes: laboratory measurements to real time measurements with an *in situ* electrochemical analyzer (ISEA). Marine Chemistry.

Lyons, T.W., 1997. Sulfur isotopic trends and pathways of iron sulfide formation in upper Holocene sediments of the Black Sea. Geochimica et Cosmochimica Acta 61, 3367–3382.

Lyons, T.W., Berner, R.A., 1992. Carbon–sulfur–iron systematics of the uppermost deep-water sediments of the Black Sea. Chemical Geology 99, 1–27.

Lyons, T.W., Kashgarian, M., 2005. Paradigm lost, paradigm found. The Black Sea–Black Shale connection as viewed from the anoxic basin margin. Oceanography 18 (2), 86–99.

Manheim, F.T., Chan, K.M., 1974. Interstitial waters of Black Sea sediments: new data and review. In: Degens, E.T., Ross, D.A. (Eds.), The Black Sea — Geology, Chemistry, and Biology. Am. Assoc. Pet. Geol. Mem., vol. 20, pp. 155–180.

Mitropolsky, A.Yu., Bezborodov, A.A., Ovsyany, E.I., 1982. Geochemistry of the Black Sea, vol. 144. Naukova Dumka, Kiev. (In Russian).

Murray, J.W., Top, Z., Ozsoy, E., 1991. Hydrographic properties and ventilation of the Black Sea. Deep-Sea Research 38 (Suppl. 2), S663–S689.

Murray, J.W., Konovalov, S.K., Romanov, A., Luther, G., Tebo, B., Friederich, G., Oguz, T., Besiktepe, S., Tugrul, S., Yakushev, E., 2003. 2001 R/V Knorr cruise: new observations and variations in the structure of the suboxic zone. In: Yilmaz, A. (Ed.), Oceanography of the Eastern Mediterranean and Black Sea, Proceeding of the "Second International Conference on Oceanography of the Eastern Mediterranean and Black Sea: Similarities and Differences of Two Interconnected Basins. TUBITAK Publishers, Ankara, Turkey, pp. 545–557.

Neprochnov, Yu.P., Neprochnova, A.F., Mirlin, Ye.G., 1974. Deep structure of Black Sea Basin. In: Degens, E.T., Ross, D.A. (Eds.), The Black Sea — Geology, Chemistry, and Biology. Am. Assoc. Pet. Geol. Mem., vol. 20, pp. 35–49.

Neretin, L.N., Böttcher, M.E., Jørgensen, B.B., Volkov, I.I., Lüschen, H., Hilgenfeldt, K., 2004. Pyritization processes and greigite formation in the advancing sulfidization front in the Upper Pleistocene sediments of the Black Sea. Geochimica et Cosmochimica Acta 68 (9), 2081–2093.

Ottley, C.J., Davison, W., Edmunds, W.M., 1997. Chemical catalysis of nitrate reduction by iron (II). Geochimica et Cosmochimica Acta 61 (9), 1819–1828.

Pilipchuk, M.F., Volkov, I.I., 1974. Behavior of molybdenum in processes of sediment formation and diagenesis in Black Sea. In: Degens, E.T., Ross, D.A. (Eds.), The Black Sea — Geology, Chemistry, and Biology. Am. Assoc. Pet. Geol. Mem., vol. 20, pp. 542–553.

Popescu, I., Lericolaisb, G., Paninc, N., Wongd, H.K., Droz, L., 2001. Late Quaternary channel avulsions on the Danube deep-sea fan, Black Sea. Marine Geology 179 (1–2), 25–37.

Postma, D., 1990. Kinetics of nitrate reduction by detrital Fe(II)-silicates. Geochimica et Cosmochimica Acta 54, 903–908.

Postma, D., Appelo, C.A.J., 2000. Reduction of Mn-oxides by ferrous iron in a flow system: column experiment and reactive transport modeling. Geochimica and Cosmochimica Acta 64 (7), 1237–1247.

Postma, D., Jakobsen, R., 1996. Redox zonation: equilibrium constraints on the Fe(III)/SO4-reduction interface. Geochimica et Cosmochimica Acta 60, 3169–3175.

Richard, D., 1997. Kinetics of pyrite formation by the H_2S oxidation of iron (II) monosulfide in aqueous solutions between 25 and 125C: the rate equation. Geochimica et Cosmochimica Acta 61, 115–134.

Rickard, D., Luther III, G.W., 1997. Kinetics of pyrite formation by the H_2S oxidation of iron(II) monosulfide in aqueous solutions between 25 and 125C: the mechanism. Geochimica et Cosmochimica Acta 61, 135–147.

Ross, D.A., Degens, E.T., MacIlvaine, J., 1970. Black Sea: recent sedimentary history. Science 170, 163–165.

Rozanov, A.G., Volkov, I.I., Yagodinskaya, T.A., 1974. Forms of iron in surface layer of Black Sea sediments. In: Degens, E.T., Ross, D.A. (Eds.), The Black Sea — Geology, Chemistry, and Biology. Am. Assoc. Pet. Geol. Mem., vol. 20, pp. 532–541.

Schaller, T., Moor, H.C., Wehrli, B., 1997. Sedimentary profiles of Fe, Mn, V, Cr, As and Mo as indicators of benthic redox conditions in Baldeggersee. Aquatic Sciences 59, 345–361.

Şengör, A.M.C., Tüysüz, O., İmren, C., Sakınç, M., Eyidoğan, H., Göorür, N., Le Pichon, X., Rangin, C., 2005. The North Anatolian Fault: a new look. Annual Review of Earth and Planetary Sciences 33, 37–112.

Shimkus, K.M., Trimonis, E.S., 1974. Modern sedimentation in Black Sea. In: Degens, E.T., Ross, D.A. (Eds.), The Black Sea — Geology, Chemistry, and Biology. Am. Assoc. Pet. Geol. Mem., vol. 20, pp. 249–278.

Strakhov, N.I., 1963. About some new data on the Black Sea sediments diagenesis. Lithology and Mineral Deposits 1, 7–27.

Sundby, B., Silverberg, N., 1981. Pathways of manganese in an open estuarine system. Geochimica et Cosmochimica Acta 45 (3), 293–307.

Taillefert, M., Bono, A.B., Luther III, G.W., 2000. Reactivity of freshly formed Fe(III) in synthetic solutions and (pore)waters: voltammetric evidence of an aging process. Environmental Science & Technology 34, 2169–2177.

Thamdrup, B., Rosselló-mora, R., Amann, R., 2000. Microbial manganese and sulfate reduction in Black Sea shelf sediments. Applied and Environmental Microbiology 66, 2888–2897.

Theberge, S.M., Luther III, G.W., 1997. Determination of the electrochemical properties of a soluble aqueous FeS species present in sulfidic solutions. Aquatic Geochemistry 3, 191–211.

Vainshteyn, M.B., Tokarev, V.G., Shakola, V.A., Lein, A.Yu., Ivanov, M.V., 1986. The geochemical activity of sulfate reducing bacteria in sediments in the western part of the Black Sea. Geochemistry International 1, 110–122.

Van der Zee, C., Van Raaphorst, W., 2004. Manganese oxide reactivity in North Sea sediments. Journal of Sea Research 52, 73–85.

Volkov, I.I., 1964. Iron sulfide nodules in the Black Sea sediments: formation and chemical composition (in Russian). Trudy Instituta Okeanologii Im. P.P. Sirsova 67, 101–134 (In Russian).

Volkov, I.I., Fomina, L.S., 1974. Influence of organic material and processes of sulfide formation on distribution of some trace elements in deep-water sediments of Black Sea. In: Degens, E.T., Ross, D.A. (Eds.), The Black Sea — Geology, Chemistry, and Biology. Am. Assoc. Pet. Geol. Mem., vol. 20, pp. 456–476.

Wijsman, J.W.M., Middelburg, J.J., Heip, C.H.R., 2001a. Reactive iron in Black Sea sediments: implications for iron cycling. Marine Geology 172, 167–180.

Wijsman, J.W.M., Middelburg, J.J., Herman, P.M.J., Bottcher, M.E., Heip, C.H.R., 2001b. Sulfur and iron speciation in surface sediments along the northwestern margin of the Black Sea. Marine Chemistry 74, 261–278.

Wijsmana, J.W.M., Herman, P.M.J., Middelburg, J.J., Soetaert, K., 2002. A model for early diagenetic processes in sediments of the continental shelf of the Black Sea. Estuarine, Coastal and Shelf Science 54, 403–421.

Wilkin, R.T., Arthur, M.A., 2001. Variations in pyrite texture, sulfur isotope composition, and iron systematics in the Black Sea: evidence for Late Pleistocene to Holocene excursions of the O_2–H_2S redox transition. Geochimica et Cosmochimica Acta 65, 1399–1416.

Wilkin, R.T., Arthur, M.A., Dean, W.E., 1997. History of water-column anoxia in the Black Sea indicated pyrite framboid size distributions. Earth and Planetary Science Letters 148, 517–525.